Journal of
Water & Climate Change

IWA PUBLISHING

Journal of Water and Climate Change Vol 14 No 9, 3071 doi: 10.2166/wcc.2023.156

Climate stress impacts on the reservoir inflows: a decision-scaling and IHACRES modeling approach in South Korean basins

Taehyeong Kim and Boosik Kang *

Department of Civil & Environmental Engineering, Dankook University, Yongin, Republic of Korea
*Corresponding author. E-mail: bskang@dankook.ac.kr

BK, 0000-0002-5246-6588

ABSTRACT

This study employed the Decision-Scaling (DS) approach and the IHACRES (Identification of unit Hydrographs And Component flows from Rainfall) long-term runoff model to investigate the impact of composite changes in rainfall and temperature on dam inflows at Chungju dam, Yongdam dam, Hapcheon dam, and Seomjingang dam basins. By analyzing flow regimes, rainfall scenarios, and temperature scenarios, the study revealed crucial insights into dam inflow and its response to climate stressors. The findings demonstrated that the rate of inflow increase in the study basins exceeded the rate of rainfall increase, indicating the significance of basin storage effects in contributing to runoff generation. The analysis of rainfall changes by quantile highlighted the dominant influence of the upper-high (UH) rainfall quantile, which led to higher flood inflow compared to other quantiles. Furthermore, scenarios with different rainfall patterns were compared, showcasing the predominant impact of UH quartile rainfall on the total inflow variation. The study also analyzed the runoff ratio, finding that changes in precipitation proportionally affected the runoff ratio. Overall, these insights contribute to understanding the sensitivity of dams to changes in rainfall and temperature, facilitating the development of strategies for sustainable water supply and flood management in dam systems.

Key words: climate stress scenario, decision-scaling, discharge, IHACRES, sensitivity analysis

HIGHLIGHTS

- Suggesting the methodology to minimize the risk in taking a specific number of scenarios for future climate change projection.
- 76 climate stress scenarios were developed.
- Showing the specific model (IHACRES)'s long-term runoff simulating performance.
- Evaluating IHACRES's modeling resolution for surface runoffs with respect to precipitation and temperature.
- Expanding climate stress tests for local basins in South Korea.

1. INTRODUCTION

The changes in spatio-temporal hydrological meteorological factors due to climate change are expected to increase flood and drought frequency, and climate change impact assessment needs to be performed by comprehensively considering future water demand increases and changes in hydrological meteorological factors (Lehner *et al.* 2006; Feyen & Dankers 2009; Trenberth *et al.* 2014). To analyze changes in water resources due to climate change, climate change scenarios are generally selected according to greenhouse gas emission scenarios such as IPCC (Intergovernmental Panel on Climate Change)'s Representative Concentration Pathways (RCPs), and after a downscaling process to correct the bias of the scenario, the change in streamflow is evaluated as input data for the hydrological model (Chokkavarapu & Mandla 2019). These scenarios, however, suffer from a significant limitation as they encompass a restricted number of potential outcomes, thus constraining the scope of analysis within a confined range of possibilities. Consequently, this restricted set of scenarios poses a challenge when attempting to comprehensively understand and predict the real-world complexities of climate change.

The discrepancy between the projected scenario paths and the observed climate change outcomes necessitates a reevaluation of the methodologies and assumptions employed in climate change impact studies. While the IPCC scenarios serve as

valuable tools for providing a range of plausible future scenarios, it is crucial to acknowledge that they represent simplified representations of reality. The inherent limitations in the number and diversity of scenarios offered by the IPCC can inadvertently hinder our ability to capture the full breadth of potential impacts, uncertainties, and risks associated with climate change (Maurer 2007; Hattermann *et al.* 2018; Her *et al.* 2019). In addition, there are no clear guidelines on which to choose among the various options of climate change forecasting, which are combined with numerous GCM climate model detailed techniques and carbon emission scenarios (Brown *et al.* 2019).

To address these challenges, researchers and policymakers must embrace a more comprehensive and deliberate approach to studying climate change impacts. This entails incorporating a broader range of potential scenarios, accounting for a wider array of contributing factors, and acknowledging the uncertainty inherent in climate projections. By adopting a more holistic perspective and incorporating a richer set of scenarios, we can enhance our understanding of the complex nature of climate change and foster more effective strategies for adaptation and mitigation. In this regard, Brown *et al.* (2012) proposed Decision-Scaling (DS), a procedure for identifying climate-related risks by priority using structured multi-dimensional sensitivity analysis with the establishment of a decision analysis framework. This is not a top-down impact assessment based on climate change scenario prediction, but a bottom-up impact assessment that precedes climate vulnerability assessment, often consisting of three stages: decision framing, climate stress test, and climate information-based risk assessment. In summary, the main objectives of this study are as follows:

(i) Assess the impact of climate change on hydrological and meteorological factors: The study aims to understand how climate change affects spatio-temporal hydrological and meteorological factors, leading to an increase in flood and drought frequency. It seeks to perform a comprehensive climate change impact assessment by considering future water demand increases and changes in these factors.
(ii) Overcome limitations of current climate change scenarios: The study acknowledges the limitations of existing climate change scenarios, such as the IPCC's RCPs, which offer a restricted number of outcomes. The objective is to address this constraint by incorporating a broader range of potential scenarios to capture a wider array of impacts, uncertainties, and risks associated with climate change.
(iii) Apply the DS method for climate change impact assessment: The study proposes the use of the DS method, which is a bottom-up approach that precedes climate vulnerability assessment. It involves three stages: decision framing, climate stress testing, and climate information-based risk assessment. The primary aim of the DS method is to generate pre-estimated impact simulations based on well-designed precipitation and temperature scenarios. By using this method, the study can estimate the hydrologic impacts of climate change using multiple forcing scenarios, including those beyond the IPCC scenarios.

As an example of DS evaluation, Freeman *et al.* (2020) designed a plan for future water management by evaluating the reliability of the system according to precipitation and temperature changes by entering a climate stress scenario that increased precipitation and temperature through the resilience design technique. This has the advantage of allowing the system to determine investment priorities for climate change adaptation according to the degree to which it is sensitive to climate change. The application of this data-driven evaluation method through case studies has been steadily growing in recent years, as evidenced by notable studies such as those conducted by Steinschneider *et al.* (2015), Knighton *et al.* (2017), Kim *et al.* (2019), as well as Quinn *et al.* (2020). These studies have shed light on the effectiveness and potential of the method in various contexts.

However, despite the increasing body of research in this area, there remains a noticeable gap when it comes to the application of these evaluation methods in the context of Korea's climate change impact assessment. While several international studies have demonstrated their applicability and benefits, there is a need for more localized case studies that specifically address the unique challenges and characteristics of Korea's climate and environment.

This study aims to evaluate the inflow of Chungju (CJ) Dam, Yongdam (YD) Dam, Hapcheon (HC) Dam, and Seomjingang (SJ) Dam, which play a central role in water supply and flood prevention in each water system using the DS method considering rainfall and temperature changes. The 76 climate stress scenarios were generated for each dam by year by dividing them into quartiles according to the ranking, and the changes in dam inflow were analyzed based on flow-duration criteria, rainfall, and temperature scenarios to evaluate which factors each dam is more sensitive to.

2. STUDY AREA, DATA, AND MODELING

2.1. Study areas

This study was conducted on one multipurpose dam for each water system, and a total of four places were selected, including CJ, YD, HC, and SJ basins (Figure 1). The IHACRES (Identification of unit Hydrographs And Component flows from Rainfall) model used in this study is a daily model, and rainfall and average temperature were collected per weather station through the Weather Data Open Portal (http://data.kma.go.kr) managed by the Korea Meteorological Administration. In the case of inflow, data on daily dam inflow provided by the national Water resources Management Information System (http://www.wamis.go.kr) operated by the Han River Flood Control Center were collected. The data period was from 1995 to 2014, the same period as the standard scenario of the IPCC sixth report, and in the case of YD dam, data from 2001 were used after completion of construction. Rainfall and temperature data were used by averaging the space with the Thiessen network of the target basin. Table 1 shows the basin area, annual average rainfall, annual average inflow, annual average, maximum, and normal temperature of the four dam basins, and the CJ dam basin has a relatively larger basin area (~7.5 times) and is evaluated to have relatively less precipitation among the four dams. The annual average temperature and maximum temperature were similar in the basin of the target dam, but the annual minimum temperature was evaluated to be relatively high in the HC dam basin.

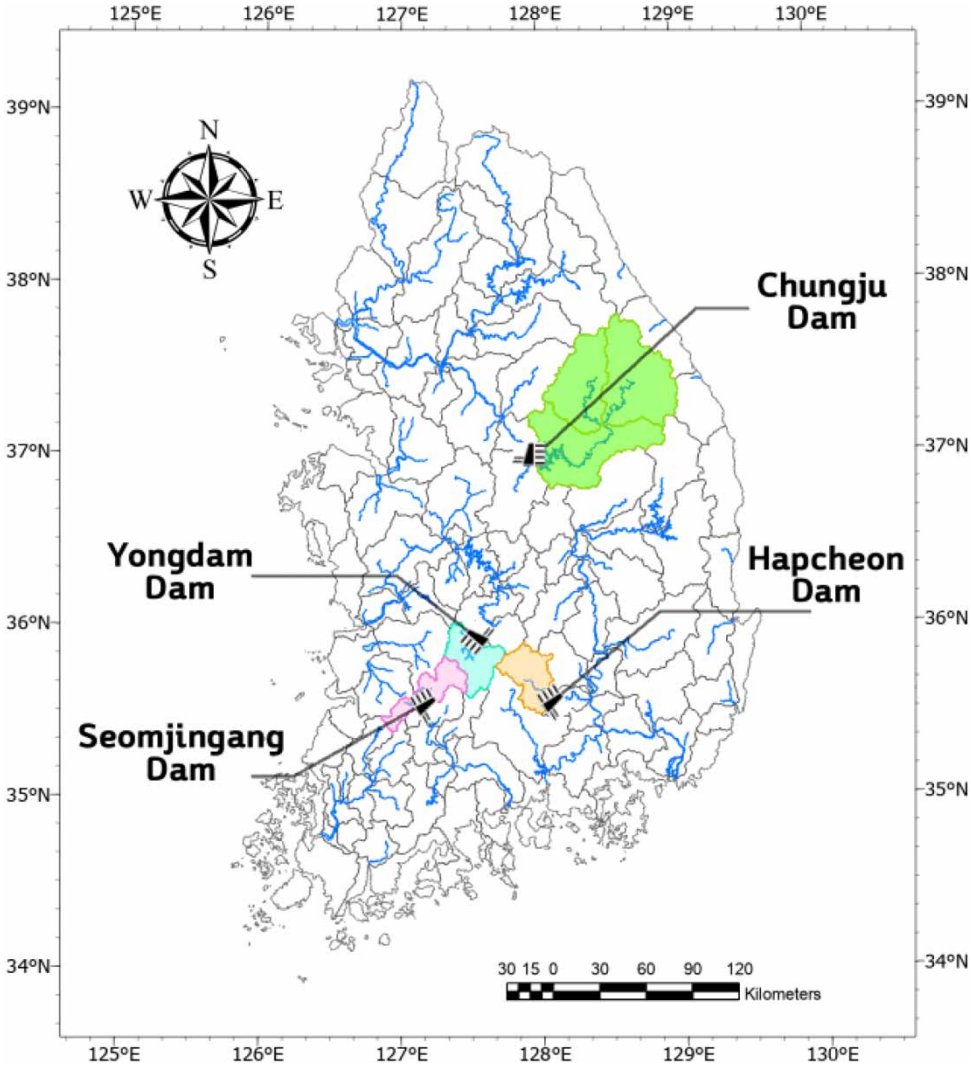

Figure 1 | Study sites used in this study.

Table 1 | Basin characteristics of the study sites

Study sites	Drainage area (Km^2)	Mean annual precipitation (mm)	Mean annual discharge (Mm^3/year)	Mean/Max/Min temperature (°C)
Chungju (CJ) dam (in Han River basin)	6,648.0	1,296.39	5,396	11.22/28.2/ − 12.1
Yongdam (YD) dam (in Geum River basin)	930.0	1,409.64	787	11.30/27.4/ − 10.0
Hapcheon (HC) dam (in Nakdong River basin)	928.9	1,359.35	682	11.97/27.9/ − 7.3
Seomjingang (SJ) dam (in Seomjin River basin)	763.5	1,424.43	616	11.11/27.3/ − 10.1

2.2. DS for climate sensitivity

Most of the existing approaches to climate change impact analysis are top-down techniques based on the GCM predictions on the top (Wilby & Dessai 2010), which first forecast climate change and downscale the output to the spatial and temporal scale of the hydrological model before evaluating the performance of the water resources system model. However, the future greenhouse gas emission scenarios are hypothetical ones, and considering this emission scenario, the climate-simulating GCM inherently contains uncertainties due to deterministic chaos characteristics, which must include significant uncertainties in regional climate predictions. The DS technique proposed to compensate for these drawbacks is a bottom-up technique that evaluates climate change vulnerabilities by analyzing sensitivity to a wide range of climate conditions through preselected evaluation indicators (Brown *et al.* 2012). The DS technique cannot completely eliminate climate change uncertainty, but it can play a role as a decision tool to preemptively identify which factors of climate change are sensitive to and to respond to future climate changes without relying on specific future climate predictions.

Figure 2 shows the steps for evaluating the DS technique used in this study. First, the method of creating a climate stress scenario to reflect the characteristics of rainfall in Korea, which is concentrated during the monsoon season, is as follows: (1) The monthly average value by year is calculated using daily precipitation data, and the ranking diagram is prepared by sorting them in descending order according to size. Then, after calculating the average of the months with the same ranking, a representative hydrological distribution diagram of the baseline scenario was prepared, and (2) the monthly precipitation change was set by dividing it into quartiles according to the ranking to ± 10, 20, and 50%. The 50% rainfall change is a value that increases the maximum rainfall change in the climate change scenario and was used only for the purpose of showing the limit value. 19 rainfall scenarios including reference scenarios were generated for each target dam basin (Table 2), and (3) the temperature change was changed at 1 °C intervals from +0 to 3 °C (Table 3), resulting in 76 ($=19 \times 4$) climate stress scenarios per dam. After simulating the inflow using the generated climate stress scenario as input data to the IHACRES model,

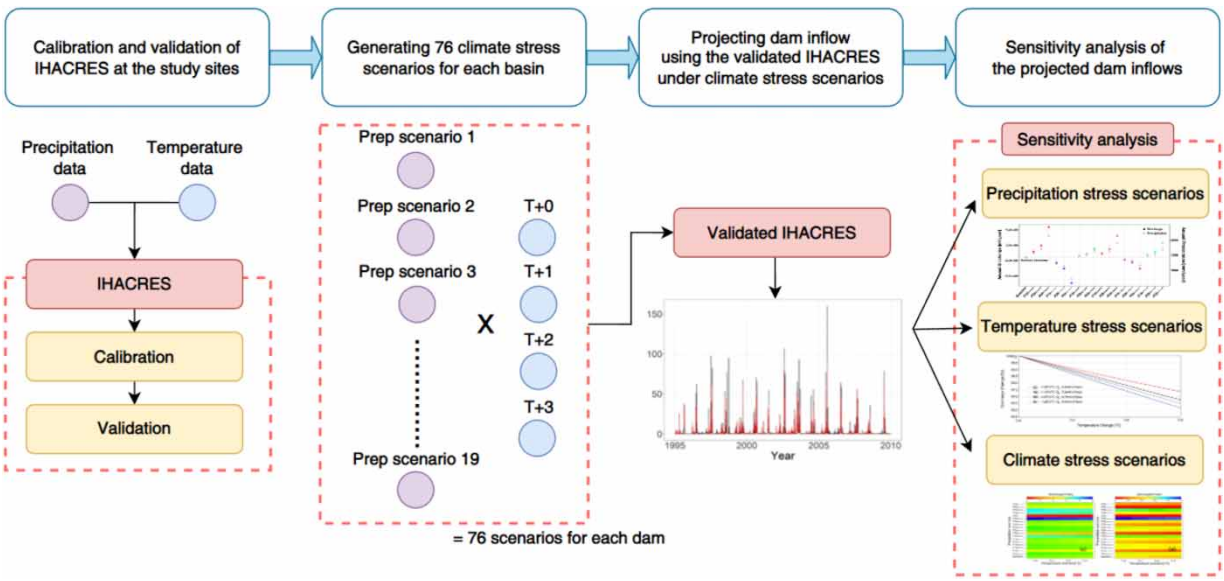

Figure 2 | Scheme for DS (Decision-Scaling) procedures used in this study.

Table 2 | Precipitation change scenarios using the quantile rank-based classification

	Quantile Rank				
Scenarios	**UH (Upper High)**	**MH (Middle High)**	**ML (Middle Low)**	**LL (Lower Low)**	**Symbolic expression**
Baseline	–	–	–	–	P × ×× ×
1	+10/20/50%	+10/20/50%	+10/20/50%	+10/20/50%	*P* + ++ +
2	−10/20/50%	−10/20/50%	−10/20/50%	−10/20/50%	P————
3	–	+10/20/50%	+10/20/50%	-	P × ++ ×
4	+10/20/50%	–	–	+10/20/50%	*P* + ×× +
5	−10/20/50%	+10/20/50%	+10/20/50%	−10/20/50%	P– + +–
6	+10/20/50%	−10/20/50%	−10/20/50%	+10/20/50%	*P* +––+

Table 3 | Temperature stress scenarios based on the baseline scenario

Temperature change	+0 °C	+1 °C	+2 °C	+3 °C
Symbolic expression	T + 0 (Baseline)	T + 1	T + 2	T + 3

the flow rate of each dam basin was evaluated based on the change in the inflow rate during rainfall and temperature changes. Through this process, each dam was evaluated to be more sensitive to the factors of climate change.

2.2.1. Long-term rainfall-runoff mode (IHACRES)

As a reservoir inflow prediction model according to the climate stress scenario, the long-term rainfall-runoff model, IHACRES, presented by Jakeman *et al.* (1990) was used (Figure 3). This is a model designed to comprehensively take the advantages of physical and conceptual models, which requires a small amount of input data and has the advantage of testing a number of scenarios as an open source code model. The IHACRES model consists of a non-linear module that converts rainfall into effective rainfall and a linear module that converts effective rainfall into outflow. This study used IHACRES' Catchment Moisture Definition (CMD) model embedded in hydromad R package as a nonlinear module of the IHACRES

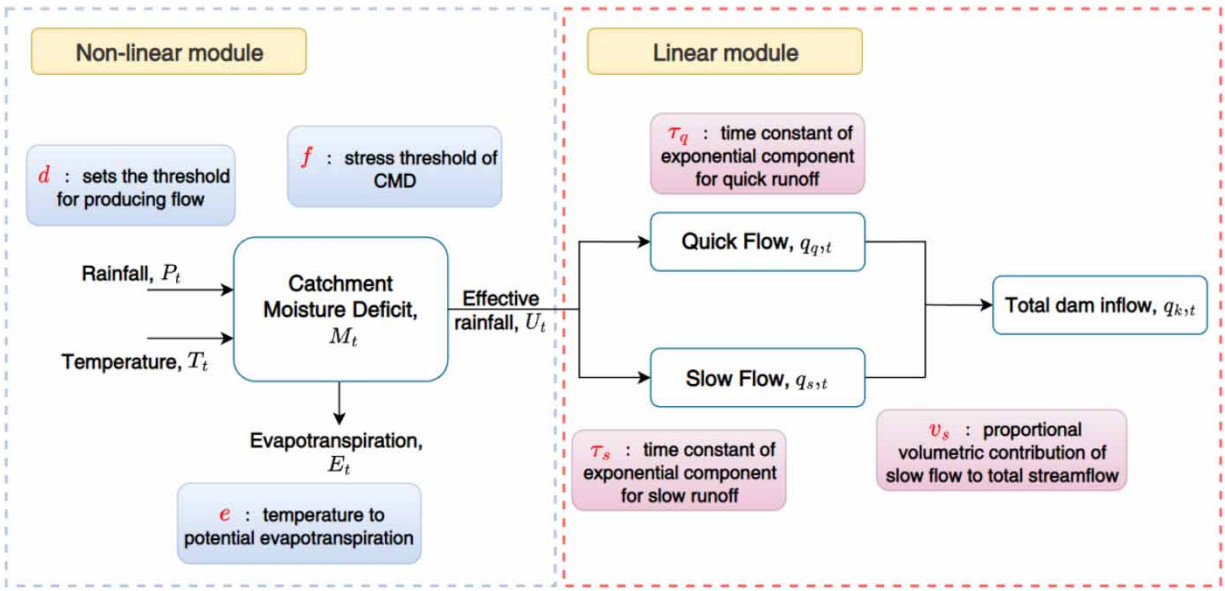

Figure 3 | Schematic diagram of IHACRES and six parameters used in this study (Modified from Evans 2003).

model. The CMD was first presented in the work of Jakeman *et al.* (1990) and Evans & Jakeman (1998), but Croke & Jakeman (2004) presented improved techniques and are used in a way that is embedded in current software.

The CMD is a technique for calculating the effective rainfall using rainfall and temperature as input data. Potential evaporation is calculated from temperature, and converted into actual evaporation and considered as a loss from the basin. The effective rainfall is obtained from the water balance equation as shown in Equation (1).

$$U_t = P_t - M_{t-1} + M_f \tag{1}$$

where U_t is the effective rainfall at time t, P_t is the rainfall at time t, and M_{t-1} is the Catchment Moisture Deficit (CMD) at time t–1.

In a nonlinear module, a tentative value of M is calculated before actual evaporation is considered. This is expressed as M_f, as shown in Equation (2). This can be derived from the mass conservation equation of $dU = dP + dM$. The detail derivation process is presented in the work of Croke & Jakeman (2004).

$$M_f = \begin{cases} M_{t-1}\exp\left(-\dfrac{P_t}{d}\right), & \text{if } M_{t-1} < d \\ d\,exp(-\left[\dfrac{P_t - M_{t-1} - d}{d}\right], & \text{if } d \le M_{t-1} < d + P_t \\ M_{t-1} - P_t, & \text{if } M_{t-1} \ge d + P_t \end{cases} \tag{2}$$

where d is the parameter indicating the limit value of CMD.

The CMD is calculated from the water balance equation as shown in Equation (3).

$$M_t = M_{t-1} - P_t + E_{T,t} + U_t \tag{3}$$

Equation (4) shows the relationship between the increase rate between rainfall and effective rainfall in this process as the soil approaches saturation over time.

$$\frac{\mathrm{d}U}{\mathrm{d}P} = 1 - f(M) = 1 - \min\left(1, \frac{M}{d}\right) \tag{4}$$

The function $f(M)$ is required to satisfy the following conditions to express this rainfall-flow relationship (Croke & Jakeman 2004).

1. The $f(M)$ has a value between 0 and 1.
2. When M is zero (i.e., when the soil is saturated), $f(0) = 0$.
3. The $f(M)$ is monotonically increased when $0 \le M \le d$.
4. $f(M) = 1$ when $M > d$.
5. $\int_{M_1}^{0} \frac{dx}{f(x)} = \infty$ when $M_1 > 0$.

As a function satisfying these conditions, $f(x) = \min\left[1, \frac{x}{d}\right]$ was used for deriving the Equation (2). The equation for calculating potential evaporation using temperature is shown in Equation (5).

$$E_{T,t}^{p} = e \times T_t \tag{5}$$

where e is a dimensionless parameter that converts temperature into latent evapotranspiration. The actual evaporation is calculated from the potential evaporation calculated previously as shown in Equation (6) and is a parameter indicating the ratio of the flow rate to the threshold value of the evapotranspiration. By using threshold parameters and reducing the dependence of the parameters on other parameters, the uncertainty of the results could be minimized, which makes it easier to calibrate

the model (Dye & Croke 2003).

$$E_{T,t} = E_{T,t}^{P} \times h(M_k) = E_{T,t}^{P} \times \left\{1,\ \exp\left[2\left(1 - \frac{M_f}{f \times d}\right)\right]\right\} \tag{6}$$

Like $f(M)$, the function h(M) is required to select a function that satisfies the following conditions (Croke & Jakeman 2004).

1. $f(M_k) = 1$ when $M_k \leq g$.
2. The $f(M)$ is monotonically increased when $M_k > g$.
3. $\lim_{M_k \to \infty} h(x) = 0$.

As a function satisfying these conditions, $h(x) = \min\{1,\ \exp[2(1 - (M_f/(f \times d)))]\}$ was used. A linear module is a module that converts an effective rainfall into a runoff, and expresses a basin runoff by configuring a linear reservoir in parallel or in series. The total runoff is divided into direct runoff and slow runoff, as shown in Equations (7)–(9).

$$q_{k,t} = q_{q,t} + q_{s,t} \tag{7}$$

$$q_{q,t} = -\alpha_q q_{q,t-1} + \beta_q U_t \tag{8}$$

$$q_{s,t} = -\alpha_s q_{s,t-1} + \beta_s U_t \tag{9}$$

where $q_{k,t}$, $q_{q,t}$, $q_{s,t}$ and refer to total outflow (mm/day), direct outflow (mm/day), and base outflow (mm/day), respectively, and the parameters α_q, α_s, β_q, β_s are calculated according to the parameters varying with time (Equations (10)–(12)).

$$\tau_q = -\frac{1}{\ln(\alpha_q)} \tag{10}$$

$$\tau_s = -\frac{1}{\ln(\alpha_s)} \tag{11}$$

$$v_s = 1 - v_q = \frac{\beta_s}{(1 + \alpha_s)} \tag{12}$$

where, τ_q is the time constant (–) of the direct runoff, τ_s is the time constant (-) of the baseflow, v_s is the ratio of the direct to the total runoff, and v_q is the ratio of the baseflow to the total runoff. When v_q is determined, v_s is determined or has an opposite relationship. Accordingly, the parameters (α_q, α_s, β_q, β_s) of the linear module may be replaced with three parameters (τ_q, τ_s, v_s). In this study, the range of parameters was selected based on previous studies, as shown in Table 4.

2.2.2. Sensitivity analysis

To analyze the flow regime changes throughout the year, the daily flow rates during the reference scenario were sorted in descending order and analyzed by day. The flow regime analysis was conducted using the average daily flow rates corresponding to each flow-duration criteria of drought flow (355 days), low flow (275 days), normal flow (185 days), high flow (95 days) and flood flow (10 days). In addition, based on the results derived from the climate stress scenario as an input value in the

Table 4 | The ranges of parameters used in IHACRES

Parameters	Definition	Range	
		Min	Max
d	Threshold of the watershed water shortage index generated by inflow	50	550
e	Temperature to potential evapotranspiration factor	0.01	1.5
f	Stress threshold of watershed water shortage index as a percentage of d	0.01	3
τ_s	Time constant of exponential component for slow runoff	5	100
τ_q	Time constant of exponential components for rapid runoff	0	5
v_s	Ratio of base runoff to total runoff	0	1

Table 5 | Optimized IHACRES parameters obtained in this study for each basin

Basin	d	e	f	τ_s	τ_q	v_s
CJ	56.96	0.1352	1.2569	100	2.9652	0.1501
YD	64.70	0.1705	0.8189	34.5757	1.6579	0.2162
HC	74.24	0.1593	0.9061	100	1.8205	0.2179
SJ	60.96	0.2049	0.8272	100	1.8169	0.0904

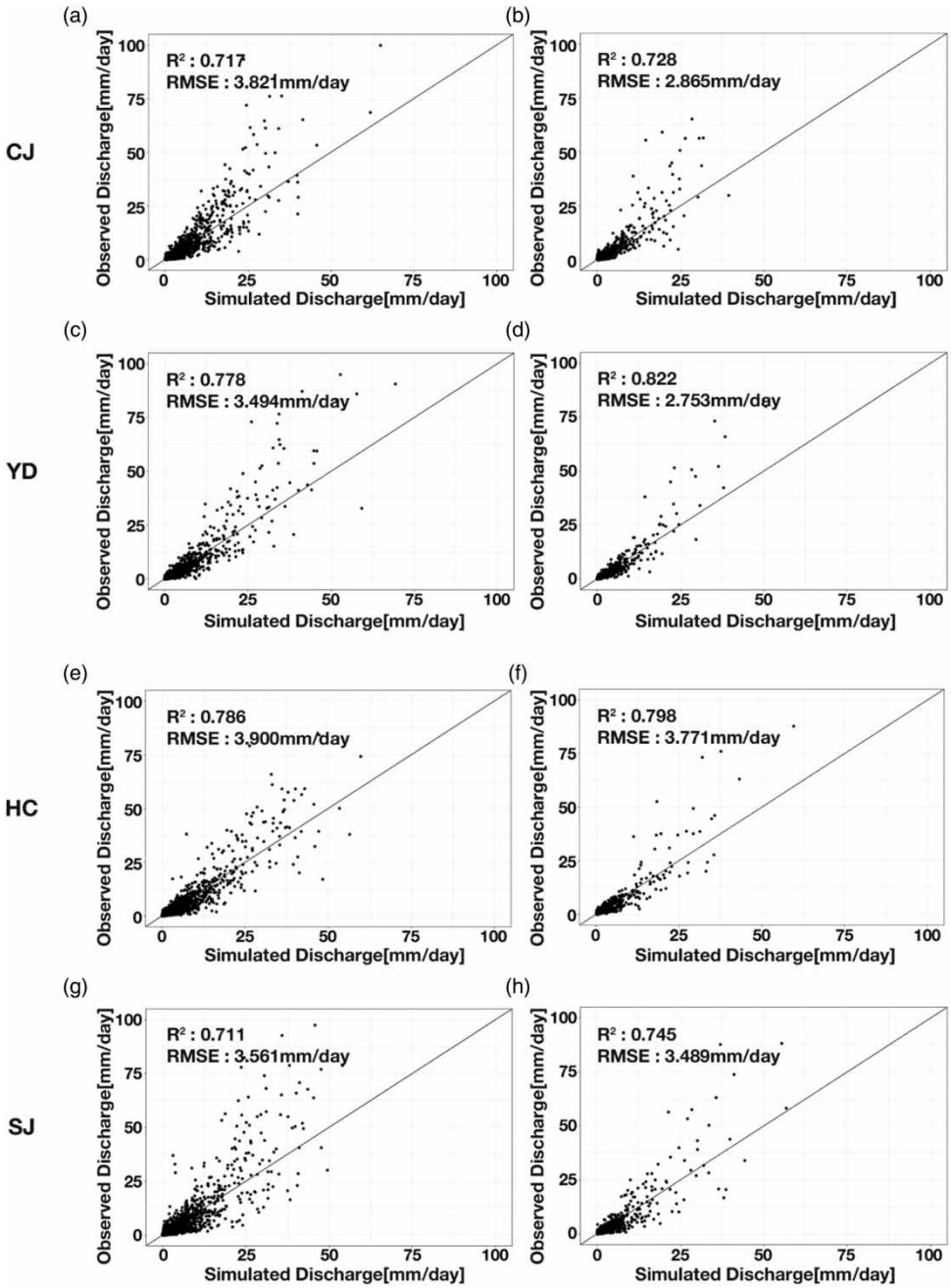

Figure 4 | Comparisons between simulated and observed discharges during the calibration period (left column) and the validation period (right column) at CJ, YD, HC, and SJ basins.

runoff model, the sensitivity of each dam is evaluated by analyzing the change in inflow with respect to the rainfall and temperature changes.

3. APPLICATION AND RESULTS

3.1. IHACRES modeling and calibration

In this study, the optimal parameters were derived by comparing the observed and simulated flow rates based on the coefficient of determination using the multi-start and pre-sampling options of hydromad (Table 5). During the reference years (1995–2014), 1995–2009 was set as the model's calibration period, 2010–2014 as the model's validation period. In the case of the YD dam with completion in 2000, 2001–2010 was set as the calibration period and 2011–2014 as the validation period. In Figure 4, the inflow amount of each dam during the calibration and validation period is shown in a scatter graph. The coefficient of determination (R^2) and root mean square error (RMSE) were used as the evaluation index. When the observed and simulated values match, the R^2 represents a value of 1, and RMSE is an index that determines the error between the observed and simulated values, and it can be judged that the closer to 0, the less the error. In all dams, it was confirmed that the calibration period had a good evaluation index between 0.71 and 0.82 and RMSE between 2.7 and 3.9 mm/day.

The flow regime curve was calculated in Figure 5 to further analyze the observed flow rate during the baseline period and the inflow simulated by IHACRES. The observed value was expressed as a straight line and the simulated value was expressed as a dotted line. In the basins of CJ and HC, the simulated flow rate was found to be almost similar in all sections of the flow regime curve. On the other hand, in YD and SJ, the simulated flow rate was similar to the observation results in flood, high- and low-flow regime, but the simulated flow rate was calculated relatively high in the drought flow regime. Although the simulated flow rate was over-estimated in the low to drought flow regime (approximately 0.1 mm/day or less), there is an observation limit for a flow rate close to zero, and it can be seen that it is difficult to accurately simulate. Even if there is a difference between observation and simulated inflow in some flow regime curve sections, the IHACRES model is feasible for reproducing past dam inflow and is considered sufficiently available for analysis of inflow due to climate stress.

3.2. Inflow analysis based on the rainfall stress scenario

The evaluation of annual inflow change for the target dam was conducted using 19 rainfall stress scenarios. The results depicted in Figure 6(a)–6(d) illustrate the annual average dam inflow based on the rainfall stress scenario. Notably, the rate of inflow increase was found to exceed the rate of rainfall increase. This pattern was observed consistently across all basins, with minimal variation between them (Table 6). Specifically, under the $P+++$ scenario, a 10% increase in rainfall resulted in an inflow increase ranging from 16.5 to 17.5% compared to the reference scenario. Moreover, with a 20% increase in rainfall, the inflow escalated by 33.3–35.2%. Conversely, in the P——— scenario, a 10% decrease in rainfall led to an inflow reduction of 16.1–17.2% relative to the reference scenario. These fluctuations exhibited a similar range to those observed in

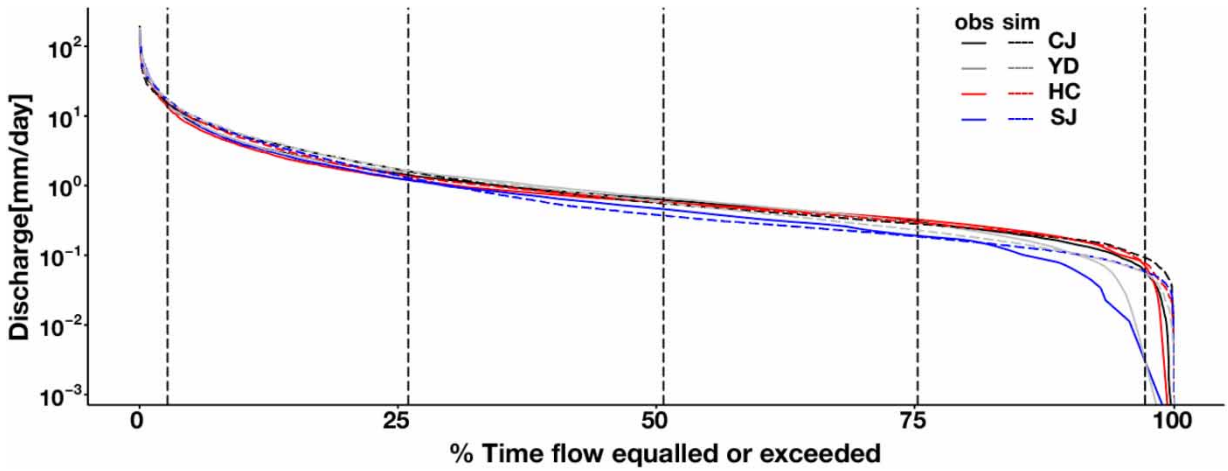

Figure 5 | Flow-duration curves for CJ, YD, HC, and SJ dam basins. The solid and dashed lines represent observed and simulated discharges, respectively.

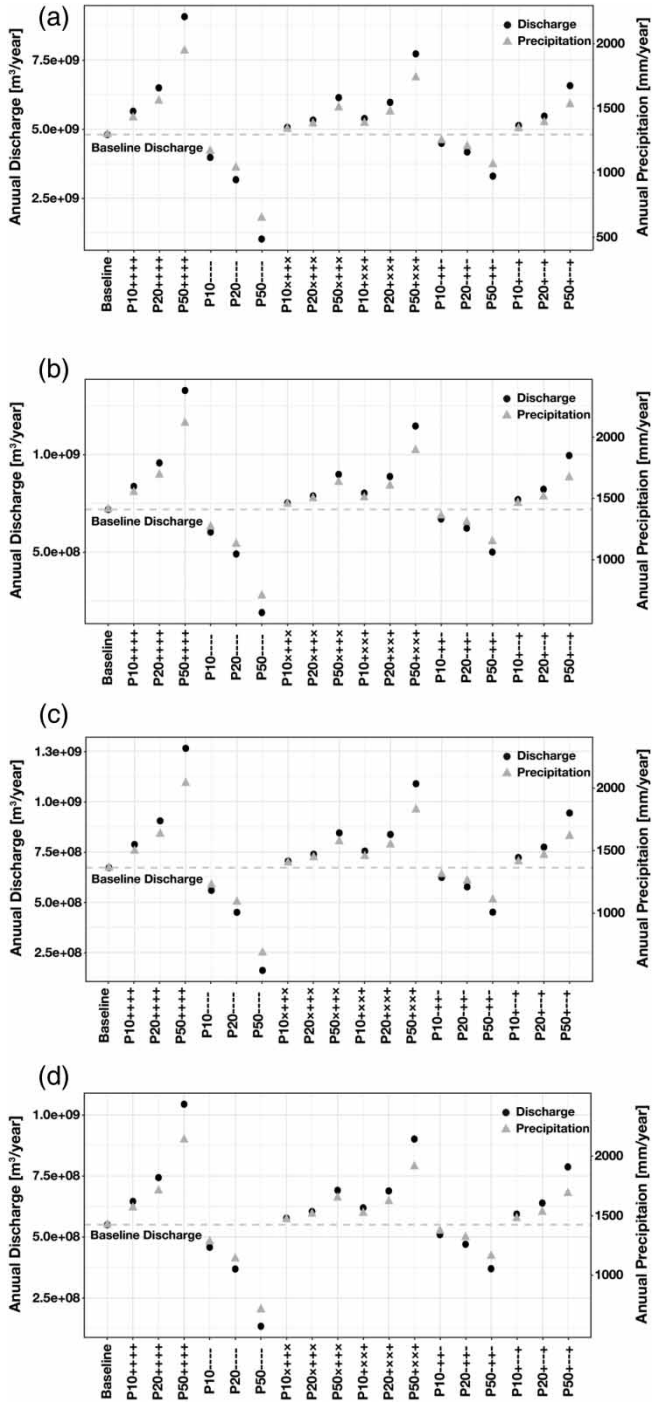

Figure 6 | Mean annual discharges (left *y*-axis) and mean annual precipitation (right *y*-axis) under precipitation stress scenarios (*x*-axis) at (a) CJ, (b) YD, (c) HC, and (d) SJ basins.

the $P+++$ scenario, albeit with slightly smaller declines that did not reach statistical significance. This outcome can be attributed to the storage effect of a basin, wherein a portion of the generated rainfall is retained in the ground soil layer, while the remaining effective rainfall generates land surface flow. Consequently, the increase rate of effective rainfall becomes greater than the increase rate of total rainfall, which is represented as the greater rate of change in dam inflow.

Subsequently, the impact of rainfall changes by quantile on total runoff variation was analyzed. Analysis was conducted based on the $P+\times+$ scenario, where rainfall increased for the upper-high (UH) and lower-low (LL) quantiles, and the

Table 6 | Rate of change in dam inflow with respect to baseline scenario

	Rate of Change (%)							
	CJ		YD		HC		SJ	
Scenario	±10%	±20%	±10%	±20%	±10%	±20%	±10%	±20%
$P+++$	17.5	35.2	16.5	33.3	17.2	34.7	17.3	35.0
P———	−17.2	−34.0	−16.1	−31.7	−16.8	−33.0	−16.8	−33.1
P × ++ ×	5.4	10.9	4.8	9.6	4.9	9.9	4.8	9.8
$P+\times\times+$	12.1	24.2	11.7	23.5	12.3	24.6	12.5	25.1
P– + +–	−6.6	−13.1	−6.8	−13.3	−7.2	−14.2	−7.5	−14.6
$P+--+$	6.8	13.8	7.1	14.5	7.5	15.2	7.9	16.1

P × ++× scenario, where rainfall increased for the middle-high (MH) and middle-low (ML) quantiles. Under the $P+\times\times+$ scenario, a 10% increase in rainfall compared to the standard scenario resulted in an inflow increase of 11.7–12.2%, while a 20% increase in rainfall showed a rise of 23.53–25.14%. Conversely, the P × ++× scenario led to an inflow increase of 4.8–5.4% for a 10% rainfall increase and an increase of 9.66–10.90% for a 20% rainfall increase. Notably, when the precipitation increase was applied to the UH quantile, the flood inflow became relatively higher than the overall increase in total inflow. Specifically, the $P+\times\times+$ scenario demonstrated a 13.5–14.1% increase in flood inflow compared to the reference scenario for a 10% rainfall increase, and a 26.8–28.8% increase for a 20% rainfall increase.

When examining changes in low flow, CJ, HC, and SJ basins exhibited greater increases in low flow under the $P+\times\times+$ scenario compared to the P × ++× scenario, whereas the YD basin showed the opposite outcome. Furthermore, when considering the normal flow, HC and SJ inflows showed a larger increase in the $P+\times\times+$ scenario compared to the P × ++× scenario, while CJ and YD basins exhibited the opposite pattern. These findings confirm that changes in UH quantile rainfall have a more prevailing effect on the total inflow of dams and overall range of flow durations. Additionally, the increase or decrease in rainfall during the monsoon season emerges as a significant factor influencing the overall inflow change due to the concentrated nature of rainfall in Korea during this period.

Furthermore, when comparing the $P+--+$ scenario and the P– + +– scenario, the $P+----+$ scenario demonstrated an inflow increase of 6.8–7.9% compared to the reference scenario for ±10% change of rainfall. Conversely, the P– + +– scenario exhibited a decreasing trend, with inflow decreasing by 6.6–7.5% compared to the reference scenario for ±10% change of rainfall. This implies that even though the rainfall in the median (MH and ML) quartile increases, the total inflow decreases if the rainfall in the upper (UH) quartile decreases. Additionally, the average annual rainfalls in the P– + +– and $P+--+$ scenarios are almost similar and the $P+--+$ scenario shows just 7% higher than the P– + +– scenario. However, when rainfall changes ±20% in the P– + +– scenario, the inflow decreased by 13.1–14.6%, whereas the $P+--+$ scenario showed an increase of 13.8–16.1%. This finding indicates that the change in rainfall within the UH quantile predominates in influencing the variation of total inflow, to the extent of displaying opposite rates of change.

In the case of the runoff ratio (U_t/P_t), it can be observed that precipitation increase leads to a proportional increase (Table 7). Under the $P+++$ scenario, the runoff ratio ranges from 53.9 to 59.1% in the 10% precipitation increase scenario, and from 56.9 to 62.3% in the 20% precipitation increase scenario. Conversely, in the P——— scenario with a 20% precipitation decrease, the runoff ratio drops to only 40.6–46.8%. The average runoff ratios for the P– + +– and $P+--+$ scenarios with a 10% increase or decrease in precipitation, but with similar annual precipitation, were 51.7 and 55.4%, respectively.

3.3. Inflow analysis based on the temperature stress scenario

Figure 7 shows the average annual inflow rate change rate of each dam when the reference scenario is increased at 1 °C intervals from temperature 0 to 3 °C. As the temperature increased by 1 °C, the change in dam inflow was evaluated as −1.08%/°C, −1.16%/°C, −0.87%/°C, and −1.28%/°C, respectively, for CJ, YD, HC, and SJ basins. Although the difference between the research areas was small, the HC showed the smallest and the SJ showed the highest rate of change. The dam inflows compared to rainfall were evaluated as 55.7% (CJ), 54.8% (YD), 53.1% (HC), and 50.6% (SJ), and SJ was evaluated to have a relatively small value. In SJ, which has the smallest dam inflow compared to rainfall, the change in dam inflow according

Table 7 | Runoff ratios by scenario

	Runoff ratios (%)							
	CJ		YD		HC		SJ	
Scenario	±10%	±20%	±10%	±20%	±10%	±20%	±10%	±20%
$P+++$	59.1	62.3	58.0	60.9	56.7	59.7	53.9	56.9
P———	50.9	40.6	51.1	46.8	49.3	44.6	46.8	42.4
P × ++ ×	56.5	57.7	55.7	56.6	54.3	55.2	51.4	52.3
$P+\times\times+$	58.1	60.5	57.4	59.6	55.9	58.4	53.3	55.7
P– + +–	53.6	51.8	53.1	51.4	51.4	49.5	48.6	46.7
$P+--+$	57.1	58.8	56.6	58.5	55.2	57.1	52.7	54.7

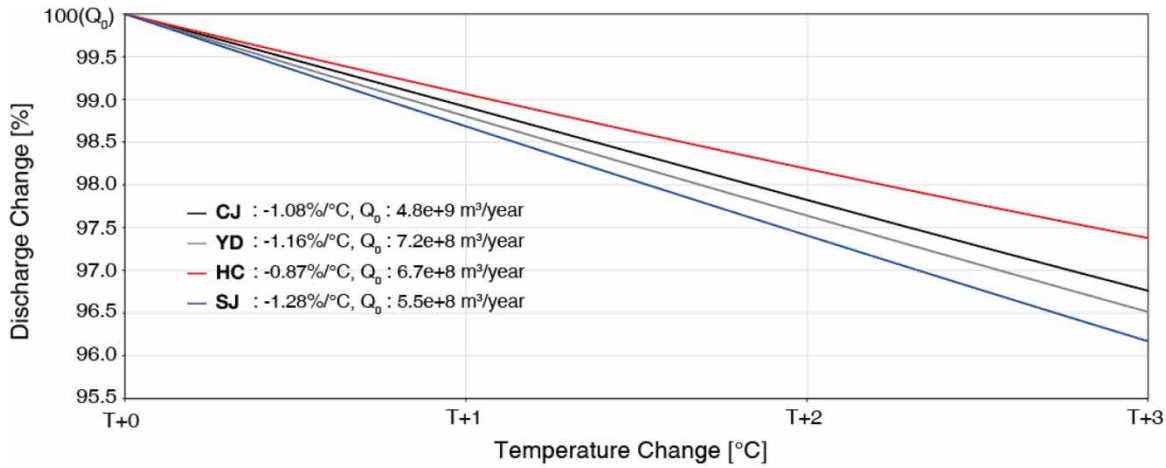

Figure 7 | Percentage changes in discharges under temperature stress scenarios compared to the baseline scenario at CJ, YD, HC, and SJ. Q_0 represents mean annual discharge under the baseline scenario.

to temperature change is the largest. The review of whether these results have a significant hydrometeorological causal relationship seems to be an issue to be conducted in depth in the future. However, compared to the results of the rainfall stress scenario conducted in this study, the change in inflow to temperature was relatively insignificant in terms of absolute quantity.

3.4. Inflow analysis based on the climate stress scenario

Figure 8 shows the change in runoff according to the climate stress scenario considering composite changes in rainfall and temperature. Figures 8(a)–8(d) show the rate of change in low flow regime among the flow regime analysis results for the runoff, and Figures 8(e)–8(h) show the rate of change in flood flow regime compared to the reference scenario. Since the results of the 50% rainfall increase/decrease scenario show extreme results compared to other scenarios, they were excluded from Figure 8 to increase visibility. In the $P+++$ scenario, when rainfall increases by 10%, the storage rate in all dams is 20.7–23.4%, the rate of change with temperature is −0.9–4.6%/°C, the rate of change with temperature is 14.3–16.2%, and the rate of change with temperature is −0.03 to 1.17%/°C. In addition, the average inflow decreasing rates with respect to the unit increase of temperature for the low-water regime are 3.87, 0.86, 2.66, and 1.34%/°C for CJ, YD, HC and SJ, respectively. Likewise, those for the high water regime show 0.06, 1.03, 0.10, and 1.05%/°C for CJ, YD, HC and SJ, respectively. Compared to YD and SJ, CJ and HC show a relatively large variation in low and flood flow regime depending on temperature, suggesting that the sensitivity to climate stress may be different for each dam when it is low and high flow regimes. Therefore, it is judged that measures for problems that may arise due to future climate change should be individually established in other dams through sensitivity analysis to climate stress.

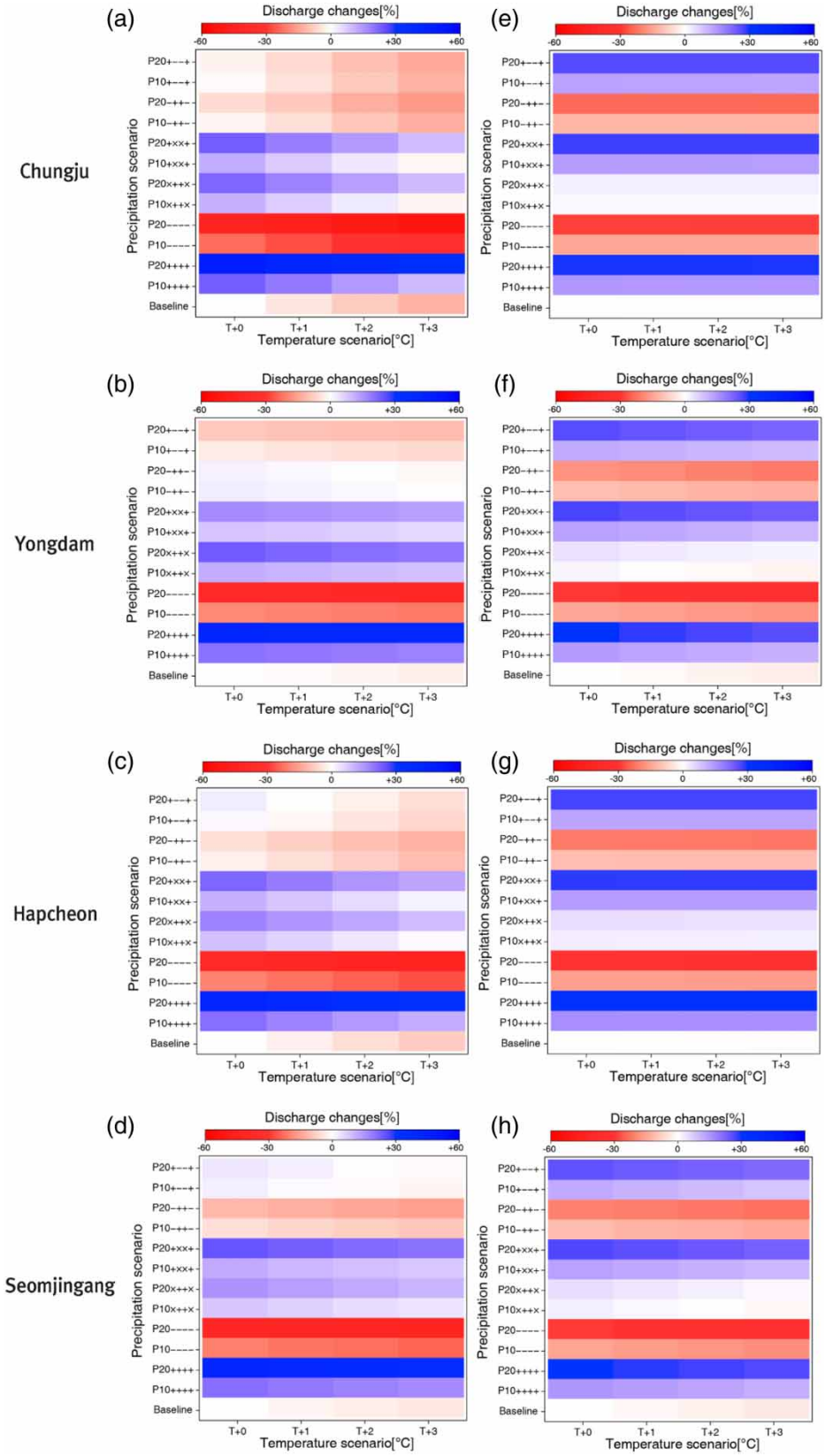

Figure 8 | Low-water inflow (left column) and flood-water inflow (right column) under climate stress scenarios at CJ, YD, HC, and SJ basins.

4. CONCLUSION

In this study, the DS approach was employed to investigate the impact of composite changes in rainfall and temperature on dam inflow. By utilizing the DS structure and the IHACRES long-term runoff model, the study analyzed changes in dam inflow considering flow regime analysis, rainfall scenarios, and temperature scenarios. The major findings shed light on several important aspects of dam inflow and its response to climate stressors.

Firstly, the study revealed the storage effects of the basins, indicating that the rate of inflow increase in the study basins exceeded the rate of rainfall increase. This observation suggests that the increase in effective rainfall, which contributes to runoff generation, surpasses the increase in total rainfall. The storage effect of the basins plays a crucial role in retaining a portion of the generated rainfall in the ground soil layer, resulting in a higher rate of change in dam inflow.

Secondly, the analysis of rainfall changes by quantile emphasized the predominant impact of the UH rainfall quantile. Increases in rainfall for the UH quantile, as well as the LL quantile, led to higher flood inflow compared to the overall increase in total inflow. On the other hand, increases in rainfall for the MH and ML quantiles resulted in a smaller increase in inflow. These findings highlight the significance of UH quantile rainfall changes in influencing the total inflow of dams and the range of flow durations.

The study also examined the changes in low flow and normal flow in different basins. It was found that the basins of CJ, HC, and SJ experienced greater increases in low flow under the scenario with increased UH and LL quantile rainfall ($P+\times\times+$), while the YD basin showed the opposite outcome. Regarding normal flow, the HC and SJ basins exhibited larger increases under the $P+\times\times+$ scenario, while the CJ and YD basins displayed the opposite pattern. These observations underline the influence of changes in UH quantile rainfall on the total inflow of dams and the range of flow durations.

Furthermore, the study compared scenarios with different rainfall patterns. When comparing the $P+--+$ scenario and the P–$+$ $+$– scenario, it was evident that a decrease in rainfall in the UH quartile led to a decrease in total inflow, even if there was an increase in rainfall in the median (MH and ML) quartile. The change in rainfall within the UH quantile had a predominant influence on the variation of total inflow, resulting in opposite rates of change.

Lastly, the study analyzed the runoff ratio in response to precipitation changes. It found that an increase in precipitation led to a proportional increase in the runoff ratio. The $P++++$ scenario with a 10% precipitation increase resulted in a runoff ratio ranging from 53.9 to 59.1%, while a 20% increase led to a ratio between 56.9 and 62.3%. Conversely, the P–––– scenario with a 20% precipitation decrease showed a lower runoff ratio ranging from 40.6 to 46.8%. Comparing scenarios with a $\pm$10% variation in precipitation but similar annual precipitation, the average runoff ratios were 51.7 and 55.4%, respectively.

Overall, these findings provide valuable insights into the sensitivity of dams to changes in rainfall and temperature. They emphasize the importance of considering different factors, such as storage effects, quantile-specific rainfall changes, and their implications for low flow, normal flow, and the runoff ratio, in evaluating dam inflow and understanding its variations. These findings contribute to the understanding of climate change impacts on water resources management and can aid in developing strategies for sustainable water supply and flood management in dam systems.

ACKNOWLEDGEMENTS

This research was supported by the National Research Foundation of Korea (NRF) funded by the Ministry of Science and ICT (No. NRF-2021K1A3A1A20003375).

DATA AVAILABILITY STATEMENT

All relevant data are included in the paper or its Supplementary Information.

CONFLICT OF INTEREST

The authors declare there is no conflict.

REFERENCES

Brown, C., Ghile, Y., Laverty, M. & Li, K. 2012 Decision scaling: linking bottom-up vulnerability analysis with climate projections in the water sector. *Water Resources Research* **48** (9), W09537. https://doi.org/10.1029/2011WR011212.

Brown, C., Steinschneider, S., Ray, P., Wi, S., Basdekas, L. & Yates, D. 2019 Chapter 12 Decision Scaling (DS): decision support for climate change. In: *Decision Making Under Deep Uncertainty From Theory to Practice*. Springer, pp. 255–287. https://doi.org/10.1007/978-3-030-05252-2.

Chokkavarapu, N. & Mandla, V. R. 2019 Comparative study of GCMs. RCMs, downscaling and hydrological models: a review toward future climate change impact estimation. *SN Applied Sciences* **1** (12), 1698. https://doi.org/10.1007/s42452-019-1764-x.

Croke, B. F. & Jakeman, A. J. 2004 A catchment moisture deficit module for the IHACRES rainfall-runoff model. *Environmental Modelling & Software* **19** (1), 1–5. https://doi.org/10.1016/j.envsoft.2003.09.001.

Dye, P. J. & Croke, B. F. 2003 Evaluation of streamflow predictions by the IHACRES rainfall-runoff model in two South African catchments. *Environmental Modelling & Software* **18** (8–9), 705–712. https://doi.org/10.1016/S1364-8152(03)00072-0.

Evans, J. P. 2003 Improving the characteristics of streamflow modeled by regional climate models. *Journal of Hydrology* **284**, 211–227. https://doi.org/10.1016/j.jhydrol.2003.08.003.

Evans, J. P. & Jakeman, A. J. 1998 Development of a simple, catchment-scale, rainfall-evapotranspiration-runoff model. *Environmental Modelling & Software* **13** (3–4), 385–393. https://doi.org/10.1016/S1364-8152(98)00043-7.

Feyen, L. & Dankers, R. 2009 Impact of global warming on streamflow drought in Europe. *Journal of Geophysical Research: Atmospheres* **114**. https://doi.org/10.1029/2008JD011438.

Freeman, S. S. G., Brown, C., Cañada, H., Martinez, V., Nava, A. P., Ray, P., Rodriguez, D., Romo, A., Tracy, J., Vázquez, E., Wi, S. & Boltz, F. 2020 Resilience by design in Mexico city: a participatory human-hydrologic systems approach. *Water Security* **9**, 100053. https://doi.org/10.1016/j.wasec.2019.100053.

Hattermann, F., Vetter, T., Breuer, L., Buda, S., Daggupati, P., Donnelly, C., Fekete, B., Flörke, M., Gosling, S., Hoffmann, P., Liersch, S., Masaki, Y., Motovilov, Y., Müller, C., Samaniego, L., Stacke, T., Wada, Y. & Krysnaova, V. 2018 Sources of uncertainty in hydrological climate impact assessment: a cross-scale study. *Environmental Research Letters* **13** (1). https://doi.org/10.1088/1748-9326/aa9938.

Her, Y., Yoo, S. H., Cho, J., Hwang, S., Jeong, J. & Seong, C. 2019 Uncertainty in hydrological analysis of climate change: multi-parameter vs. multi-GCM ensemble predictions. *Scientific Reports* **9** (1), 4974. https://doi.org/10.1038/s41598-019-41334-7.

Jakeman, A. J., Littlewood, I. G. & Whitehead, P. G. 1990 Computation of the instantaneous unit hydrograph and identifiable component flows with application to two small upland catchments. *Journal of Hydrology* **117**, 275–300. https://doi.org/10.1016/0022-1694(90)90097-H.

Kim, D., Chun, J. A. & Choi, S. J. 2019 Incorporating the logistic regression into a decision-centric assessment of climate change impacts on a complex river system. *Hydrology and Earth System Sciences* **23** (2), 1145–1162. https://doi.org/10.5194/hess-23-1145-2019.

Knighton, J., Steinschneider, S. & Walter, M. T. 2017 A vulnerability-based, bottom-up assessment of future riverine flood risk using a modified peaks-over-threshold approach and a physically based hydrologic model. *Water Resources Research* **53** (12), 10043–10064. https://doi.org/10.1002/2017WR021036.

Lehner, B., Döll, P., Alcamo, J., Henrichs, T. & Kaspar, F. 2006 Estimating the impact of global change on flood and drought risks in Europe: a continental, integrated analysis. *Climatic Change* **75** (3), 273–299. https://doi.org/10.1007/s10584-006-6338-4.

Maurer, E. P. 2007 Uncertainty in hydrologic impacts of climate change in the Sierra Nevada, California, under two emissions scenarios. *Climatic Change* **82** (3), 309–325. https://doi.org/10.1007/s10584-006-9180-9.

Quinn, J. D., Hadjimichael, A., Reed, P. M. & Steinschneider, S. 2020 Can exploratory modeling of water scarcity vulnerabilities and robustness be scenario neutral? *Earth's Future* **8** (11), e2020EF001650. https://doi.org/10.1029/2020EF001650.

Steinschneider, S., Wi, S. & Brown, C. 2015 The integrated effects of climate and hydrologic uncertainty on future flood risk assessments. *Hydrological Processes* **29** (12), 2823–2839. https://doi.org/10.1002/hyp.10409.

Trenberth, K. E., Dai, A., Van Der Schrier, G., Jones, P. D., Barichivich, J., Briffa, K. R. & Sheffield, J. 2014 Global warming and changes in drought. *Nature Climate Change* **4** (1), 17–22. https://doi.org/10.1038/nclimate2067.

Wilby, R. L. & Dessai, S. 2010 Robust adaptation to climate change. *Weather* **65** (7), 180–185. https://doi.org/10.1002/wea.543.

First received 25 March 2023; accepted in revised form 8 August 2023. Available online 25 August 2023